J. Fluid Mech. (1980), *vol.* 97, *part* 4, *pp.* 759–769
Printed in Great Britain

Two-dimensional linear and nonlinear stern waves

By H. J. HAUSSLING

David W. Taylor Naval Ship Research and Development Center,
Bethesda, Maryland 20084

(Received 6 March 1979 and in revised form 12 June 1979)

Numerical solutions are presented for the unsteady irrotational flow generated by the movement of the stern of a two-dimensional semi-infinite body at the free surface of an incompressible fluid. When separation occurs other than at a sharp trailing edge, the location of the separation point is computed as part of the solution. Linear and nonlinear results are compared. It is shown that for draught-based Froude numbers greater than 3 the nonlinear effects are negligible for most practical purposes while for Froude numbers less than three these effects can be significant.

1. Introduction

The hydrodynamic performance characteristics of a ship are largely determined by the details of the flow near the bow and the stern. For this reason, numerous efforts have been made to analyse bow and stern flows. Baba (1976) discusses experimental and theoretical studies of such flows. He carried out a theoretical analysis of stern waves in which the ship's hull was replaced by an assumed free-surface pressure distribution and near-field expansions were used with linearized free-surface boundary conditions. More exact application of both hull and free-surface conditions has so far been limited to two dimensions. Dagan & Tulin (1972) used perturbation expansions to study the nonlinear problem of steady bow flow past a semi-infinite two-dimensional flat-bottomed body. Vanden-Broeck & Tuck (1977) and Vanden-Broeck, Schwartz & Tuck (1978) extended this work to nonlinear stern flows and included higher-order terms in the series expansions.

To obtain solutions for transom sterns Vanden-Broeck, Schwartz & Tuck assumed that the water turns the corner at the sharp trailing edge and then rises on the transom to a stagnation point where separation occurs. Except perhaps for very low Froude numbers, a more realistic model results if the flow is assumed to separate at the corner. Haussling & Van Eseltine (1976) used such a model in a numerical study of the flow generated by two-dimensional planing bodies. Hulls without sharp trailing edges were also treated by computing the location of the separation point as part of the solution process. In such a case an additional condition is needed to assure uniqueness. For this purpose, it was required that the pressure on the wetted portion of the hull be greater than atmospheric pressure. Similar numerical techniques have now been extended to handle the nonlinear free-surface and exact hull boundary conditions. The methods have been used to compute the unsteady stern waves generated by two-dimensional semi-infinite hulls. This paper describes and compares the resulting linear and nonlinear solutions.

While this paper was in the review process it was pointed out to the author that a

0022–1120/80/4420–8710 $02.00

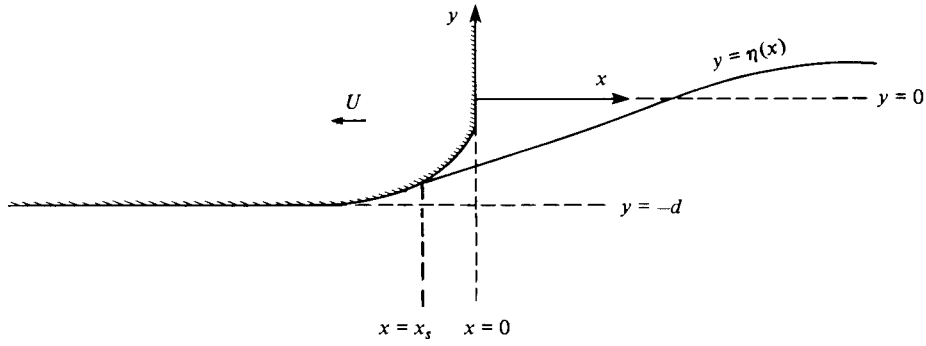

FIGURE 1. Ship stern (hatched) of draught d showing co-ordinate system, separation point at $x = x_s$, and free surface $y = \eta$.

paper by Vanden-Broeck (1980) was also under review. In his recent work Vanden-Broeck obtained numerical solutions of an integro-differential formulation for the steady nonlinear waves for a flat-bottomed hull when the flow separates at the trailing edge. He found that a steady-state nonlinear solution exists only for a draught-based Froude number greater than 2·23. The present unsteady solutions can be compared with these steady-state results of Vanden-Broeck.

2. Mathematical formulation

A study is made of the flow development resulting from the abrupt acceleration from rest to speed U of a semi-infinite ship hull in a free surface. The hull is of infinite span and of draught d as defined in figure 1. The fluid, which is infinitely deep, is initially at rest. An (x, y) co-ordinate system moves with the body and has its origin at the intersection of the stern with the undisturbed free surface. It is assumed that the flow is irrotational and that the fluid is incompressible and lacks surface tension. It is also assumed that the upper boundary of the fluid can be described at any time t by specifying y as a single-valued function of x, i.e. $y = \eta(x, t)$. This assumption is not valid if the waves approach breaking conditions. The upper fluid boundary coincides with the hull, $y = f(x)$, upstream from the separation point at $x = x_s$, and is a free boundary downstream from this point. The fluid boundary, velocities and pressure are assumed to be continuous at the separation point. When the hull has a sharp trailing edge below the undisturbed free-surface level, the flow is assumed to separate at the edge immediately after the acceleration of the hull. When there is no sharp trailing edge the initial location of the separation point is at the intersection of the hull with the undisturbed free surface. After the acceleration the separation point is free to move whether or not there is a sharp trailing edge. The location of separation is uniquely determined by two conditions. The pressure p on the hull upstream from the separation point must be greater than zero (atmospheric) and the free surface downstream from the separation point must be below the hull, $\eta(x, t) < f(x)$.

For the upper boundary elevation η and the potential ϕ for the velocity relative to a frame at rest, the dimensionless form of the initial/boundary-value problem in the moving reference frame is:

$$\phi_{xx} + \phi_{yy} = 0 \quad \text{for} \quad -\infty < x < \infty, \quad -\infty < y < \eta; \tag{1}$$

$$\eta_t = (-1-\phi_x)\eta_x + \phi_y \quad \text{for} \quad x_s(t) \leqslant x < \infty, \quad y = \eta; \tag{2}$$

$$\eta = f(x) \quad \text{for} \quad -\infty < x \leqslant x_s(t); \tag{3}$$

$$\left.\begin{aligned} \phi_t &= -\phi_x - \eta/Fr^2 - \tfrac{1}{2}(\phi_x^2+\phi_y^2) \quad \text{for} \quad x_s(t) \leqslant x < \infty \\ \nabla\phi.\mathbf{n} &= -\mathbf{i}.\mathbf{n} \quad \text{for} \quad -\infty < x \leqslant x_s(t) \end{aligned}\right\} \quad y = \eta; \tag{4, 5}$$

$$\phi_x = 0 \quad \text{for} \quad x = \pm\infty, \quad -\infty < y < \eta; \tag{6}$$

$$\phi_y = 0 \quad \text{for} \quad -\infty < x < \infty, \quad y = -\infty; \tag{7}$$

$$p > 0 \quad \text{for} \quad -\infty < x < x_s(t), \quad y = \eta; \tag{8}$$

$$\eta(x,t) \leqslant f(x) \quad \text{for} \quad x_s(t) < x \leqslant 0; \tag{9}$$

$$\phi(t=0) = 0 \quad \text{for} \quad -\infty < x < \infty, \quad -\infty < y < \eta; \tag{10}$$

$$\eta(t=0) = 0 \quad \text{for} \quad 0 < x < \infty; \tag{11}$$

$$x_s(t=0) = 0. \tag{12}$$

The subscripts x, y and t denote differentiation with respect to these variables. The characteristic length and velocity scales in the dimensionless quantities are d, the draught, and U, the speed of the hull. The Froude number is $Fr = U/(gd)^{\frac{1}{2}}$, where g is the gravitational acceleration. The unit vector normal to the hull is $\mathbf{n}$, and $\mathbf{i}$ is a unit vector in the x direction.

The pressure on the hull can be computed from the Bernoulli equation

$$p = -\phi_t - \phi_x - \tfrac{1}{2}(\phi_x^2+\phi_y^2) - y/Fr^2. \tag{13}$$

The problem can be linearized by dropping the terms $\phi_x\eta_x$ in equation (2) and $\frac{1}{2}(\phi_x^2+\phi_y^2)$ in equation (4), replacing equation (5) by $\phi_y = f_x$, and applying equations (2), (4) and (5) at $y = 0$. This linearization includes both the body and free-surface boundary conditions. The resulting problem is that of the flat-ship theory for planing surfaces. The linear theory is accurate for sufficiently small hull and free-surface slopes.

3. Method of solution

The solution technique is similar to that used by Haussling & Coleman (1979) to study nonlinear water waves generated by a submerged circular cylinder. In that work a numerically generated mapping was used to create a boundary-fitted co-ordinate system suitable for use in a finite-difference formulation. The simplicity of the geometry of the present problem allows a similar mapping to be applied exactly before the problem is discretized. The transformation

$$\xi = \exp\{c(y-\eta)\} \tag{14}$$

is applied to map the physical region in (x,y) space to a rectangular computational region in (x,ξ) space bounded below by $\xi = 0$ and above by $\xi = 1$. The parameter c can be used to control the rate of expansion of the co-ordinate system in physical space. The governing equations are transformed according to the relations

$$\begin{aligned} (\phi_x)_{y=\text{constant}} &= (\phi_x)_{\xi=\text{constant}} - c\xi\eta_x\phi_\xi, \\ \phi_y &= c\xi\phi_\xi. \end{aligned} \tag{15}$$

For instance, the Laplace equation (1) assumes the form

$$\phi_{xx}+A\phi_{\xi\xi}+B\phi_{\xi}+C\phi_{x\xi}=0, \tag{16}$$

where

$$\begin{aligned} A &= c^2\xi^2(1+\eta_x^2),\\ B &= c\xi\{c(1+\eta_x^2)-\eta_{xx}\},\\ C &= -2c\xi\eta_x, \end{aligned} \tag{17}$$

and where x derivatives now imply that ξ rather than y is being held constant. The boundary conditions (6) are applied at computational boundaries far upstream and downstream rather than at infinity. Equation (16) is replaced by a system of finite-difference equations involving the values of ϕ on a uniformly spaced system of grid points in the (x,ξ) plane. Standard second-order central differencing is used. The resulting difference equations are solved iteratively using successive over-relaxation. The calculations are vectorized on a Texas Instruments Advanced Scientific Computer (TI-ASC) through use of the 'red–black' method for sweeping the mesh (Haussling 1979).

Euler's modified method of time differencing is used to replace the free-surface boundary conditions (2) and (4) by

$$\eta_i^{n+1}=\eta_i^n+\tfrac{1}{2}\Delta t(F_{i,j=1}^{n+1}+F_{i,j=1}^n) \tag{18}$$

and

$$\phi_{i,j=1}^{n+1}=\phi_{i,j=1}^n+\tfrac{1}{2}\Delta t(G_{i,j=1}^{n+1}+G_{i,j=1}^n), \tag{19}$$

where the superscripts refer to time levels, the subscripts i and j refer to the spatial location of grid points with $j=1$ indicating the upper boundary, Δt is the time increment, and $F_{i,j}$ and $G_{i,j}$ are finite-difference approximations to the right-hand sides of (2) and (4).

The implicit equations (18) and (19) are solved iteratively for ϕ and η at the advanced time level. The iterative solution of these equations is combined with the iterative solution of equation (16). An adjustment of the surface elevation and the potential on the surface according to equations (18) and (19) is followed by an update of the Laplace equation coefficients according to equation (17) and then an adjustment of ϕ below the surface according to equation (16) and the finite-difference approximations to the boundary conditions (5)–(7). The iteration procedure is started with initial estimates of η_i^{n+1} and $\phi_{i,j}^{n+1}$ obtained by extrapolation from two previous time levels. The iterations are halted when the percentage change of η and ϕ from iteration to iteration is less than 1%. If, at the end of a time step, the pressure is negative at one or more grid points upstream from the separation point, that point is shifted upstream to eliminate the negative pressure region from the wetted surface of the hull. Alternatively, if the free surface downstream from the separation point moves upward to meet the hull, the wetted surface is extended as necessary. Thus, during the flow development, a grid point on the upper boundary can change its character between that of a hull point ($x < x_s$) and that of a free-surface point ($x > x_s$).

Although at the separation point both conditions (4) and (5) apply, only one can be enforced. Haussling & Van Eseltine (1976) found that, when the flow separates at a sharp trailing edge, the application of the hull condition (5) leads to a solution with a discontinuous pressure at the separation point. However, the application of the free-surface condition (4) at $x = x_s$ (which enforces continuity of pressure) results in

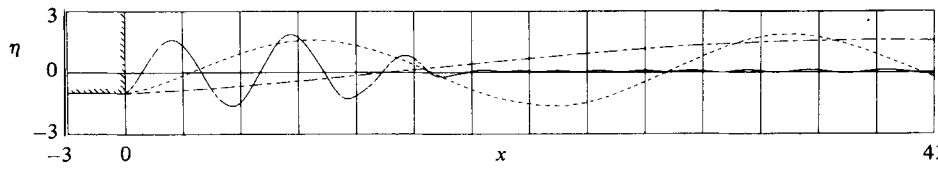

FIGURE 2. Linear surface elevations at $t = 32Fr^2$ for a flat hull.
——, $Fr = 1$; - - - -, $Fr = 2$; - · - · -, $Fr = 4$.

solutions which approximately satisfy condition (5) at $x = x_s$, and the error in satisfying this hull boundary condition can be reduced by increasing the number of points used to resolve the flow field. Thus in the present work the free-surface condition (4) is applied at $x = x_s$ and the hull condition (5) is enforced at that point only indirectly.

To eliminate the numerical instability previously encountered in such unsteady nonlinear schemes a filtering procedure is applied. After each time step new values of η_i^{n+1} and $\phi_{i,1}^{n+1}$ are computed according to the smoothing formula

$$h_i' = [-h_{i+2} - h_{i-2} + 4(h_{i+1} + h_{i-1}) + 14h_i]/16. \tag{20}$$

This filtering scheme has previously been used successfully for nonlinear water wave problems (Longuet-Higgins & Cokelet 1976; Haussling & Coleman 1979).

In the linearized case the length of the waves downstream from any disturbance is $\lambda_l = 2\pi Fr^2$. The lengths of the nonlinear waves are known to be smaller than those of the linear waves at the corresponding Froude number. For most of the calculations the computational upstream boundary was located a distance of $6\lambda_l$ from the stern and the downstream boundary was $14\lambda_l$ from the stern. For most cases twenty grid lines were used per linear wavelength in the x direction, $\Delta x = \lambda_l/20$. When higher accuracy was desirable forty grid lines were employed per wavelength. The ξ direction was resolved with twenty grid lines. The factor c in the transformation (14) was chosen to make the distance between the surface and the first grid line below the surface one-half the horizontal grid spacing. With twenty grid lines per wavelength there are 8000 grid points. This grid system was tested on a pure linear progressing wave and was found to give excellent accuracy. With a time step of $\Delta t = 0{\cdot}2Fr^2$, which is just below the experimentally determined maximum stable time step, about 160 time steps and 5 min TI-ASC central processor time were needed to calculate the flow development from the impulsive start to the time at which two essentially steady waves have developed behind the stern.

4. Results

Flat hull, linear

The hull is described by

$$y = f(x) = -1 \quad \text{for} \quad -\infty < x \leqslant 0. \tag{21}$$

If the dimensionless variables x, y and t are replaced by new variables defined by dividing the old ones by Fr^2, the linearized governing equations and boundary conditions are made independent of the Froude number. Thus the linear solutions are similar at all Froude numbers and need be computed only once. Figure 2 displays the

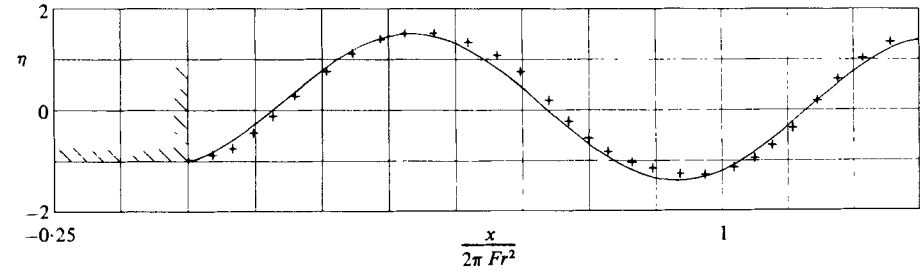

FIGURE 3. Surface elevations for a flat hull. ——, unsteady linear at $t = 144Fr^2$; +, steady state computed by Vanden-Broeck (1980).

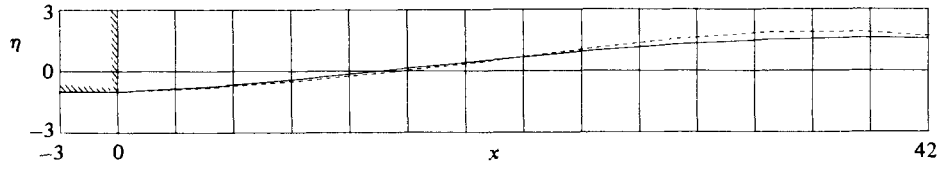

FIGURE 4. Linear and nonlinear surface elevations for a flat hull at $Fr = 4$. ——, linear; - - - -, nonlinear.

free-surface elevations for $Fr = 1$, 2, and 4 at $t = 32Fr^2$. The first two waves in each train are almost fully developed, although farther downstream transient effects still dominate. The linear wavelength $2\pi Fr^2$ is evident. The heights of the first two peaks, which are independent of Fr, are about 1·6. This number is high compared to the exact value of $\sqrt{2}$ for the far-field wave amplitude given by Vanden-Broeck. The first peak is significantly influenced by its proximity to the stern but the second peak is not. Numerical experiments have shown that the most substantial contributions to this disagreement with the exact result come from the discretization of the horizontal direction and the lack of achievement of a precise steady state in the unsteady results. The calculation of very accurate steady-state results from an unsteady formulation can often be quite time-consuming. In the present problem the final approach to steady state is gradual, with the free surface oscillating in time, with slowly diminishing amplitude, about its ultimate location. Additional calculations were carried out to $t = 144Fr^2$ with 40 instead of 20 grid lines per wavelength. Computer cost was kept down by locating the downstream boundary 2 wavelengths from the stern and replacing the far-field boundary condition (6) with the linear steady-state condition $\phi(x, y) = \phi(x + \lambda_l, y)$. These results are compared in figure 3 with points digitized from figure 1 of Vanden-Broeck (1980). The wave elevations at successive peaks and troughs downstream from the stern are 1·508, −1·399, 1·429 and −1·418, in good agreement with the exact results.

Flat hull, nonlinear

Linear and nonlinear results at $t = 512$ for $Fr = 4$ are compared in figure 4. The linear solution is quite accurate because the wave slopes involved are small. The nonlinear waves have only slightly higher peaks and a slightly shorter wavelength. The pressure on the hull is essentially the same in the two cases.

A similar comparison is made in figure 5 for $Fr = 3$. Streamlines for the nonlinear case are presented in figure 6. At this Froude number the difference between the

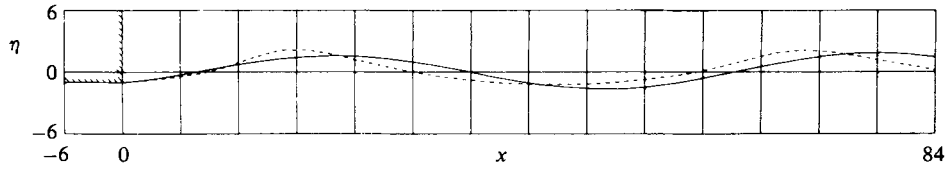

FIGURE 5. Linear and nonlinear waves for a flat hull at $Fr = 3$.
——, linear; - - - -, nonlinear.

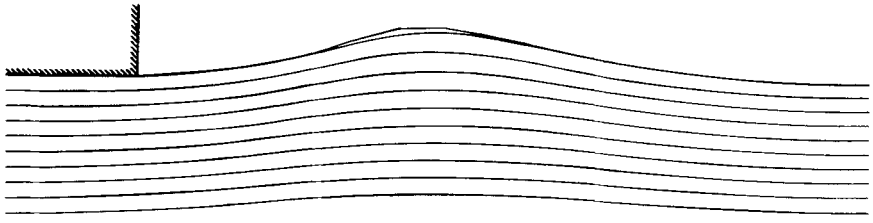

FIGURE 6. Nonlinear streamlines for a flat hull at $Fr = 3$.

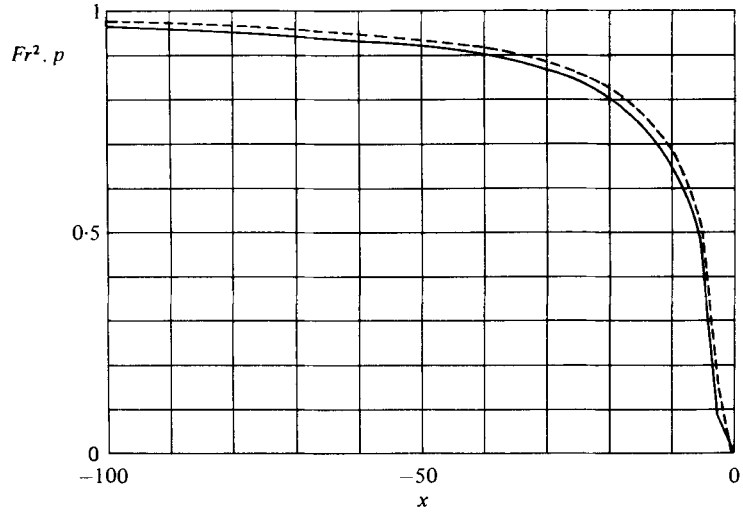

FIGURE 7. Linear and nonlinear pressure on a flat hull at $Fr = 3$.
——, linear; - - - -, nonlinear.

linear and nonlinear surface elevations is more significant than at $Fr = 4$. The wave peak elevations are increased from $y = 1{\cdot}6$ to $y = 2{\cdot}2$ by the nonlinear effects. The troughs are raised from $-1{\cdot}6$ to $-1{\cdot}2$. The wavelength is shortened by an amount which is smaller than the horizontal grid spacing and thus cannot be measured accurately. This result is consistent with the wavelength change of about 2 % for this case predicted by perturbation theory (von Kerczek & Salvesen 1974).

Figure 7 shows that, for $Fr = 3$, the nonlinear hull pressure at $t = 512$ is only slightly higher than the linear pressure.

In order to assess the size of the numerical errors both the linear and nonlinear cases were rerun to $t = 144$ with 40 instead of 20 grid lines per linear wavelength.

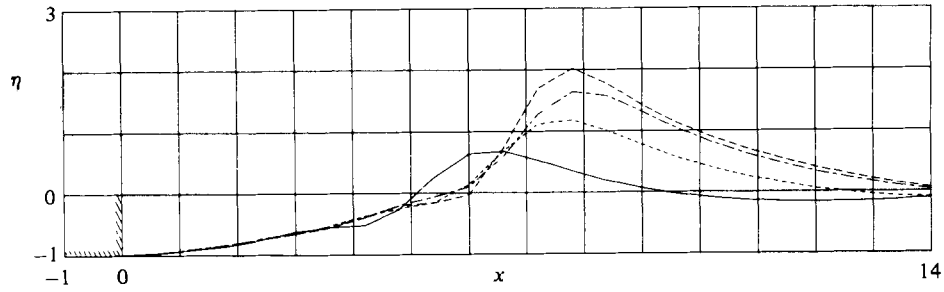

FIGURE 8. Nonlinear wave development for a flat hull with $Fr = 2$.
——, $t = 16$; - - - -, $t = 24$; – · – · –, $t = 32$; – – –, $t = 40$.

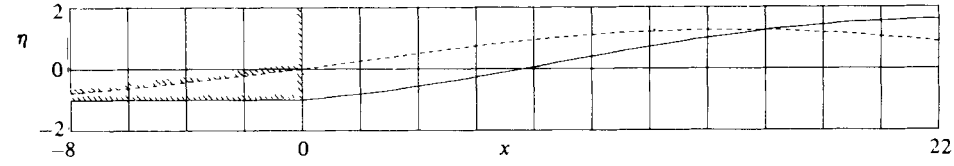

FIGURE 9. Linear surface elevations for flat and curved hulls with $Fr = 3$.

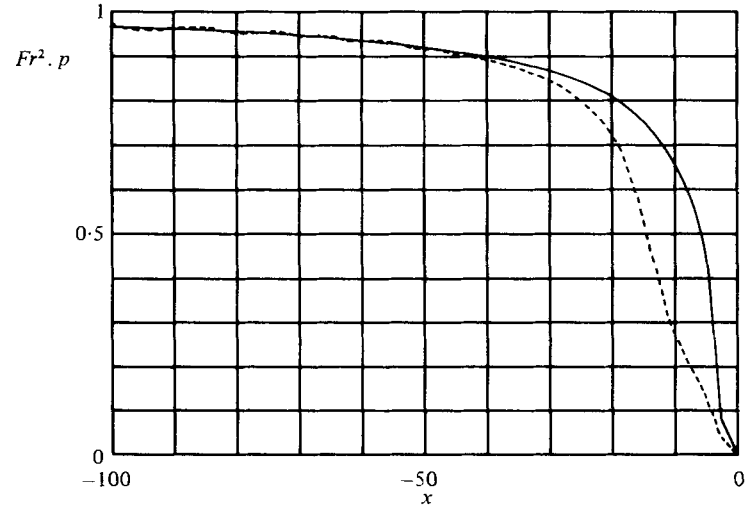

FIGURE 10. Pressure on flat and curved hulls with $Fr = 3$. ——, flat; - - - -, curved.

This doubling of the number of grid points resulted in small (5–10%) downstream shifts of the first wave peaks and similarly small reductions in the height of these peaks in both the linear and nonlinear cases. The most critical areas for resolution seem to be in the vicinity of the stern, where there is an abrupt transition from hull to free-surface conditions, and in the neighbourhood of the nonlinear wave peak, where the free surface is highly curved.

The unsteady nonlinear solutions for $Fr = 3$ and 4 give every indication of approaching, to within the numerical accuracy, the steady-state nonlinear solutions which were found by Vanden-Broeck (1980). Vanden-Broeck showed that for $Fr < 2{\cdot}23$ no

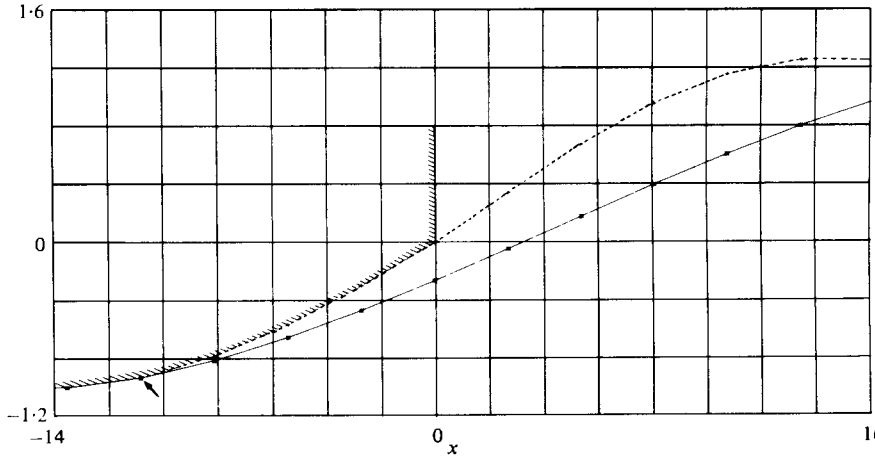

FIGURE 11. Surface elevations for curved hull. - - - -, $Fr = 3$; ——, $Fr = 4$. The arrow denotes the separation point for $Fr = 4$.

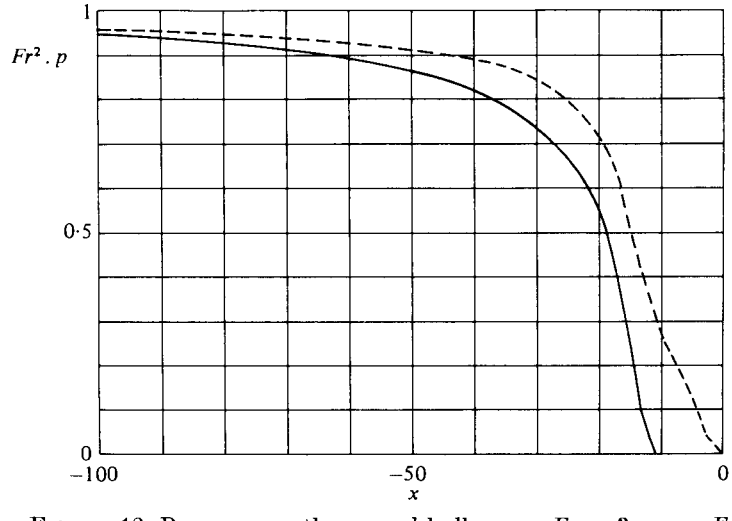

FIGURE 12. Pressures on the curved hull. - - - -, $Fr = 3$; ——, $Fr = 4$.

steady-state solution exists. However, in this lower Froude number range unsteady solutions can be obtained. Such a nonlinear flow evolution was computed for $Fr = 2$ using 40 grid lines per wavelength. Figure 8 shows the free-surface profiles at various times. A wave peak grows quickly at about $x = 8$. The upstream face of this wave steepens until accurate resolution is no longer possible with the present model. The calculations cease to converge shortly after $t = 40$. In reality, this wave would probably become a breaking stern wave. The evolution here is quite similar to that computed by Haussling & Coleman (1979) for a large-amplitude wave generated by a submerged circular cylinder.

Curved hulls

Curvature of the hull affects both the waves and the pressure on the hull. For instance, shaping the hull to conform to the expected wave shape at a particular Froude number should lower the wave height and reduce the hull pressure. The linear results for $Fr = 3$ in figures 9 and 10 show that a hull with a $\frac{1}{4}$ period sinusoidal shape near the stern

$$f(x) = -1 \qquad \text{for} \quad -\infty < x \leqslant -4{\cdot}5\pi,$$

$$f(x) = \sin(x/9) \quad \text{for} \quad -4{\cdot}5\pi < x \leqslant 0, \tag{22}$$

generates waves with amplitude 1·3 and exhibits a pressure which is indeed lower than that on the flat hull at the same Froude number. At higher Froude numbers the flow will separate before the trailing edge. At $Fr = 4$ the separation point moves forward rapidly after the acceleration of the hull. It becomes steady at $x = -10{\cdot}8$. The steady-state surface elevations for $Fr = 3$ and 4 are compared in figure 11. In this figure the vertical scale has been exaggerated. The corresponding hull pressure distributions are shown in figure 12.

5. Summary

Numerical methods have been used to analyse the unsteady linear and nonlinear waves generated by the stern of a semi-infinite two-dimensional body at the surface of a fluid. The flow was assumed to separate smoothly from the hull at a sharp trailing edge or further upstream if the hull pressure fell to zero. The linear waves for a flat-bottomed-body approach the steady state predicted for this problem by Vanden-Broeck (1980). Nonlinear effects, especially on the hull pressure, are rather small for $Fr > 3$ but are quite significant for $Fr < 3$. Locally steady-state nonlinear solutions have been obtained for $Fr = 3$ and 4. For $Fr = 2$ a transient nonlinear development was followed to a point at which the wave slope was quite large and the calculations broke down. These results are consistent with Vanden-Broeck's finding that nonlinear steady-state solutions exist only for $Fr > 2{\cdot}23$. For curved hulls solutions have been obtained by following the movement of the separation point.

This work was supported by the Numerical Naval Hydrodynamics Program at the David W. Taylor Naval Ship Research and Development Center. This program is sponsored jointly by DTNSRDC and the Office of Naval Research.

REFERENCES

BABA, E. 1976 Wave breaking resistance of ships. *Int. Seminar on Wave Resistance*, The Society of Naval Architects of Japan.

DAGAN, G. & TULIN, M. P. 1972 Two-dimensional free-surface gravity flow past blunt bodies. *J. Fluid Mech.* **51**, 529.

HAUSSLING, H. J. 1979 Boundary-fitted coordinates for accurate numerical solution of multi-body flow problems. *J. Comp. Phys.* **30**, 107.

HAUSSLING, H. J. & COLEMAN, R. M. 1979 Nonlinear water waves generated by an accelerated circular cylinder. *J. Fluid Mech.* **92**, 781.

HAUSSLING, H. J. & VAN ESELTINE, R. T. 1976 Numerical solution of planing-body problems. *David W. Taylor Naval Ship R. & D. Center Rep.* 76-0118.

KERCZEK, C. K. VON & SALVESEN, N. 1974 Numerical solutions of two-dimensional nonlinear wave problems. *10th Symp. on Naval Hydrodyn., Mass. Institute of Technology*, p. 649.

LONGUET-HIGGINS, M. S. & COKELET, E. D. 1976 The deformation of steep surface waves. 1. A numerical method of computation. *Proc. Roy. Soc.* A **350**, 1.

VANDEN-BROECK, J.-M. 1980 Nonlinear stern waves. *J. Fluid Mech.* **96**, 603.

VANDEN-BROECK, J.-M. & TUCK, E. O. 1977 Computation of near-bow or stern flows, using series expansion in the Froude number. *Proc. 2nd Int. Conf. on Numerical Ship Hydrodyn., Univ. of California, Berkeley*, p. 371.

VANDEN-BROECK, J.-M., SCHWARTZ, L. W. & TUCK, E. O. 1978 Divergent low Froude-number series expansion of non-linear free-surface flow problems. *Proc. Roy. Soc.* A **361**, 207.